HTML ABSTRACT + LINKS

Grain growth theories and the isothermal evolution of the specific surface area of snow

Loïc Legagneux, Anne-Sophie Taillandier, and Florent Domine[a)]
CNRS, Laboratoire de Glaciologie et Géophysique de l'environnement, BP 96, 38402 St. Martin d'Hères Cedex, France

(Received 15 October 2003; accepted 1 March 2004)

Quantifying the specific surface area (SSA) of snow and its variation during metamorphism is essential to understand and model the exchange of reactive gases between the snowpack and the atmosphere. Isothermal experiments were conducted in a cold room to measure the decay rate of the SSA of four snow samples kept in closed systems at $-15\,^{\circ}\mathrm{C}$. In all cases, a logarithmic law of the form $\mathrm{SSA}=B-A\ln(t+\Delta t)$ fits the SSA decrease very well, where A, B and Δt are adjustable parameters. B is closely related to the initial SSA of the snow and A describes the SSA decay rate. These and previous data suggest the existence of a linear relationship between A and B so that it may be possible to predict the decay rate of snow SSA from its initial value. The possibility that grain coarsening theories could explain these observations was investigated. The logarithmic equation was shown to be an approximation of a more general equation, that describes the time evolution of the mean grain radius R in most grain coarsening theories, such as Ostwald ripening: $\overline{R}^n-\overline{R_0}^n=Kt$. $\overline{R_0}$ is the initial mean grain radius, $\overline{R}$ is the mean grain radius, n and K are the growth exponent and the growth rate, respectively. Values of n between 2.8 and 5.0 are found. It is concluded that snow metamorphism and Ostwald ripening processes are governed by similar rules. Ostwald ripening theories predict that a steady-state regime is reached after a transient stage, but our results suggest that the steady-state regime is not reached after a few months of isothermal snow metamorphism. This last feature makes is difficult to predict the rate of decrease of snow SSA using the theory of Ostwald ripening. © *2004 American Institute of Physics.* [DOI: 10.1063/1.1710718]

I. INTRODUCTION

The snowpack is a peculiar material of interest to many scientific fields such as avalanche forecasting,[1–4] climate modeling,[5] remote sensing,[6] and, more recently, atmospheric chemistry.[7] Snow has remarkable structural properties. It is a porous material with a layered, heterogeneous, and anisotropic structure that impacts, among other things, its mechanical, optical, heat, and mass transport properties.[1] But above all, it is a dynamic medium that evolves with time.[8,9] Its transformations and the underlying mechanisms that cause them are described as a whole under the name ''metamorphism.'' Snow metamorphism can take place in the presence or in the absence of liquid water in the snowpack, leading to different physical processes. This study concentrates on the metamorphism of dry snow. Regarding wet snow metamorphism, the reader is referred to earlier work by Colbeck,[10,11] Raymond and Tusima[12] and Brun.[13]

Dry snow metamorphism originates, to a large extent, from the very high saturating vapor pressure of water. Under gradients of temperature or curvature this generates high gradients of water pressure. In response, snow grains grow or sublimate, which produces morphological changes.[11,14,15] Mechanical action of wind or fresh snow accumulation also affects she structure of this fragile porous medium. Since snowpack physical properties are related to its microstructure, they evolve at the same time, and both microstructure and physical properties then need to be studied simultaneously for a satisfactory understanding of snow metamorphism.

The relationship between grain morphology and mechanical properties of snow layers illustrates this necessity.[16] Dry snow metamorphism under high temperature gradients yields faceted crystals with few bonds,[15,17] while dry snow metamorphism under low temperature gradients yields cohesive layers of rounded grains well bonded to each other.[11]

The conditions of metamorphism determine the changes of grain shapes and sizes and thus impact the radiative properties of snow[18] in all the spectral range, from microwaves to the visible.[6] Snow emissivity has been shown to depend on fresh snow accumulation, but also on the development on the snowpack surface of faceted snow crystals called surface hoar.[19] The remote sensing community is thus directly interested in metamorphic effects and hence climate modelers, too, because they use accumulation or albedo data from satellites. Climate modelers also need to quantify the energy and mass fluxes at the air-snow interface, and therefore inside the snowpack, where they depend on the snow structure.[1–3,5,20,21]

The exchanges of water vapor between the snowpack and the atmosphere during metamorphism can also entrain trace gases dissolved in snow crystals or adsorbed on their surfaces. These processes are part of the air-snow interactions reviewed by Dominé and Shepson.[7] These authors em-

[a)]Author to whom correspondence should be addressed; electronic mail: florent@lgge.obs.ujf-grenoble.fr

 © 2004 American Institute of Physics

Downloaded 01 Jun 2004 to 132.239.1.230. Redistribution subject to AIP license or copyright, see http://jap.aip.org/jap/copyright.jsp

phasized that the surface area of the ice-air interface intervenes in each of these processes and should be considered as a central parameter. Legagneux, Cabanes, and Domine[22] confirmed this importance by measuring the specific surface area of 176 snow samples, i.e., the surface area of snow accessible to gases per unit mass. Values as high as 1580 $cm^2\,g^{-1}$ were found, with a strong correlation between snow specific surface area (SSA) and snow morphology. Since metamorphism modifies the morphology of snow, it also impacts the SSA, hence the ice-air interactions and consequently atmospheric chemistry.

SSA and metamorphism seem to be intimately related. Sokratov[23] claimed that the intensity of metamorphism increases with the SSA of snow. Cabanes, Legagneux, and Domine[24,25] showed that SSA almost always decreases along with metamorphism and proposed an empirical equation relating the rate of decrease to temperature. Despite the fact that snow SSA is clearly a major parameter for the quantification of metamorphism as well as for applications in atmospheric chemistry, the empirical equation of Cabanes and co-workers[25] is the only one available to predict its evolution in natural snow. There is thus a strong need for a physically based model of the evolution of snow SSA. Our current effort focuses on the rate of decrease of SSA under isothermal conditions. Isothermal conditions very seldom exist in natural snowpacks, where the variation of environmental parameters such as air temperature, wind, insolation, and cloud cover lead to the presence of time-variable temperature gradients.[24,25] However, isothermal experiments are easier to perform and to interpret and thus are a logical first step in our quantitative study of the rate of SSA decrease.

In a previous study,[26] we performed isothermal experiments and observed that the SSA of snow under isothermal conditions decreased with time according to Eq. (1)

$$\mathrm{SSA} = B - A\ln(t+\Delta t), \tag{1}$$

where A, B, and Δt are adjustable parameters. From these preliminary results, we observed that A and B were linearly linked for a given temperature. Flin *et al.*[27] observed the same logarithmic trend for the isothermal evolution of snow at -2 °C. Equation (1), however, cannot apply to long times, as it predicts that the SSA becomes negative. Also, the physical meaning of Δt is unclear, since it is adjusted to get the best agreement between Eq. (1) and the experimental data. The same criticism can be addressed to B which is not exactly the SSA at the beginning of the experiment but at a given time when $t+\Delta t=1$. Equation (1) and its parameters obviously suffer from a lack of physical justification and of a theoretical basis.

The purpose of this article is to move one step further towards the prediction of the rate of decrease of snow SSA under isothermal conditions. This could probably be achieved through complete three-dimensional (3D) models. Flin *et al.*[28] proposed a preliminary model of the evolution of snow morphology under isothermal evolution where the vapor fluxes are fully driven by curvature gradients. From their simulations, they were capable of qualitatively deriving the evolution of the SSA. In spite of promising results and because of computing limitations, this model at present neglects surface kinetic effects and diffusion in the vapor phase or on the surface of snow. It also needs high resolution 3D tomographic images as input data, which requires synchrotron beam time, followed by lengthy data analysis.

Another possible approach to model the rate of decrease of snow SSA is to consider it as a grain coarsening problem. Many grain coarsening theories have been developed for materials other than snow. The aim of this article is thus to test whether these theories can be applied to isothermal snow and in particular whether they can be used to justify Eq. (1) and to predict the rate of decrease of the snow SSA. To achieve this goal, we first obtained additional data on the isothermal evolution of snow SSA, in order to confirm the validity of Eq. (1), and the correlation between A and B. We then test the consistency of Eq. (1) with equations deduced from grain coarsening theories.

II. SAMPLES AND EXPERIMENT

A. Sampling

Four snowfalls were sampled during winter 2002/2003. Snowfall 1 of 7 November 2002 was sampled close to the road going to the Roche-Béranger part of the Chamrousse ski area, at an altitude of 1490 m, 15 km E-SE of Grenoble, (45°5′57″N,5°51′25″E). Snow consisted of rimed needles, columns, and dendritic crystals. The temperature of the snow surface was 0 °C. The top 2 cm were sampled directly into a stainless steel chamber used for the SSA measurements and into glass vials for subsequent microscopic observations.

Snowfall 2 of 29 January 2003 was sampled at Col de Porte, 10 km north of Grenoble, at an altitude of 1340 m in the Chartreuse range (45°12′N,5°44′E). This snow was composed of graupel, of heavily rimed large dendritic crystals and of some needles. The temperature of the snow surface was -5.6 °C.

Snowfall 3 of 3 March 2003 was sampled at Bachat-Bouloud, near the Chamrousse ski area at an altitude of 1750 m, 15 km E-SE of Grenoble (45°7′10″N,5°52′35″E). The snow consisted of fine graupel mixed with a few rimed dendritic crystals. The temperature of the snow was 0 °C. Snowfall 4 of 2 April 2003 was also sampled at Bachat-Bouloud, 2 cm under the surface where the temperature was -2.4 °C. It was composed of coarse grains of graupel 3–6 mm in diameter. All samplings were carried out during the snowfalls.

Snow was sampled carefully to minimize compaction and disturbance to its structure. A stainless steel ultrahigh vacuum container used for SSA measurements was thermalized at snow temperature, filled with snow, sealed and stored in liquid nitrogen at 77 K to prevent any evolution until they were transferred into a cold room at -15 °C.

B. Isothermal experiments

Four isothermal experiments labeled 1, 2, 3, and 4 were conducted in a cold room at -15 °C. Experiment 1 used snow from Snowfall 1 and so on. Snow sample characteristics and experimental conditions are listed in Table I, along with data on previous similar experiments from Legagneux *et al.*[26] numbered 5–9. The procedure to measure snow SSA was methane adsorption at 77 K, followed by the Brunauer–

Downloaded 01 Jun 2004 to 132.239.1.230. Redistribution subject to AIP license or copyright, see http://jap.aip.org/jap/copyright.jsp

TABLE I. Snow properties and experimental conditions. Experiments 5 to 9 are from Legagneux *et al.* (see Ref. 26).

Experiment No.	Sampling date and place	Snow crystal types	Cold room temp. °C	Snow density
1	7 November 02 Chamrousse	Rimed needles, columns, and dendritic crystals	−15	0.10
2	29 January 03 Col de Porte	Graupel, big rimed dendritic crystals, needles	−15	0.05
3	6 March 03 Bachat-Bouloud	Fine graupel, a few dendritic crystals	−15	0.10
4	2 April 03 Bachat-Bouloud	Coarse graupel, diameter 3–6 mm	−15	0.15
5	16 January 02 Col de Porte	Plates, needles, columns, dendritic crystals, capped prisms, bullet rosettes.	−15	0.075
6	6 February 02 Chamrousse	Short prisms, columns, plates, stacks of plates, various combinations with sharp angles.	−15	0.12
7	6 February 02 Chamrousse	Same as above	−4	0.12
8	21 February 02 Col de Porte	Graupel	−15	0.14
9	21 February 02 Col de Porte	Dendritic crystals, needles, columns, plates	−10	0.18

Emmett–Teller (BET) treatment of the adsorption isotherm, as described in detail by Legagneux and co-workers,[22] who estimated the reproducibility at 6% and the overall accuracy, which accounts for systematic errors of the BET treatment, at 12%. This technique does not alter the snow structure and allowed the use of the very same sample for all measurements of a given isothermal evolution.

We recently noticed that methane adsorbs not only on snow, but also on stainless steel at 77 K, which has not been taken into account in our previous articles. The surface area of the container adds to the surface area of snow, which is thus overestimated by about 0.013 m^2 in our device. The SSA is the surface area divided by the mass of snow, and the error on the SSA caused by this artifact depends on the mass of snow in the container and ranges from 25 to 100 $cm^2\,g^{-1}$. All data presented here are corrected for this bias. The vials are not transparent and we could not check for snow compaction and density changes.

III. RESULTS AND DISCUSSION

As shown in Fig. 1 the SSA always decreases with time. Equation (1) was found to fit all curves very well and Table II gives the corresponding parameters A, B, and Δt.

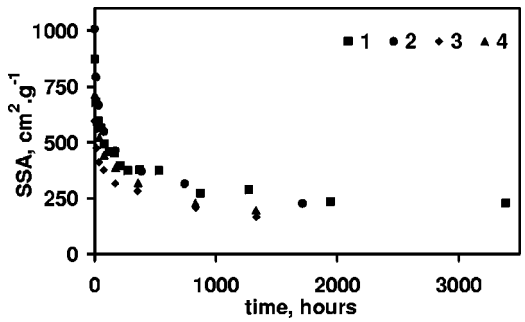

FIG. 1. Evolution with time of the SSA of snow samples 1–4, subjected to isothermal conditions at −15 °C. The longest experiment lasted 141 days; 1000 h≈42 days.

Our preliminary results[26] suggested a linear relationship between A and B at −15 °C and we were led to speculate that other linear relationships would be valid at different temperatures. This would allow the prediction of the SSA decrease from a set of curves $A=f(B,T)$ and the measurement of the initial SSA. We test this relationship at −15 °C. A is plotted against B in Fig. 2 with the data of the present work and those from our previous work.[26] The new points (circles) are aligned with the former ones (diamonds), which supports the existence of a simple linear relationship between parameters A and B at −15 °C. The equation of the linear regression is $A=0.1242\times B-19.752$. In the previous article, we had given $A=0.3416\times B-108.74$. The difference between the two equations is mostly due to the effect of methane adsorption on stainless steel that has been corrected in this article.

These results are encouraging since they have an important predictive value. The linear link between A and B at −15 °C relies on seven points, which is enough to exclude the possibility that it could be fortuitous. On the other hand, only two other data points are available, one at −4 °C and one at −10 °C, and they seem to lie on the same line. This is quite surprising since metamorphism is more intense at higher temperatures and we would therefore expect an accelerated rate of decrease of the SSA. More data are clearly

TABLE II. Fit parameters to Eq. (1): $SSA=B-ALn(t+\Delta t)$.

Expt. No.	Temperature °C	A $cm^2\,g^{-1}$	B $cm^2\,g^{-1}$	Δt Hours
1	−15	89.3	904	1.4
2	−15	117.5	1085	1.9
3	−15	70.4	682	3.4
4	−15	95.5	878	2.9
5	−15	61.7	696	18.1
6	−15	82.2	835	28.2
7	−4	68.4	691	19.5
8	−15	95.4	961	15.2
9	−10	74.7	733	100.7

Downloaded 01 Jun 2004 to 132.239.1.230. Redistribution subject to AIP license or copyright, see http://jap.aip.org/jap/copyright.jsp

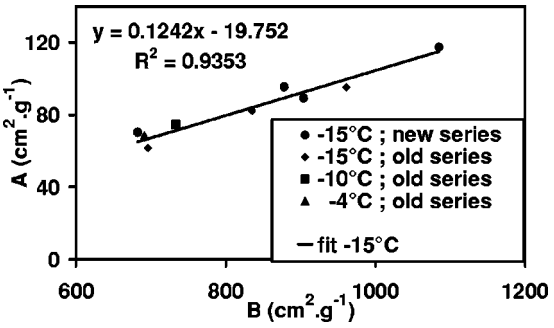

FIG. 2. Plot of parameter B vs parameter A in Eq. (1) for the nine evolutions. The new points at $-15\,^{\circ}\mathrm{C}$ (circles) are aligned with those of Legagneux *et al.* (see Ref. 26) obtained at $-15\,^{\circ}\mathrm{C}$ (diamonds). The equation of the least square fit of the data obtained at $-15\,^{\circ}\mathrm{C}$ is $A=0.1242\ B-19.752$ and its correlation coefficient is 0.9353. Data points at -10 and $-4\,^{\circ}\mathrm{C}$ lie close to this fit.

needed to test whether other linear relationships exist at different temperatures and predict the rate of SSA decrease on a wide range of temperatures.

The prediction of the rate of SSA decrease under isothermal conditions thus appears to be possible from simple empirical relationships. However, this aim will not be achieved until much more data are obtained, and isothermal experiments are time consuming. Moreover, Eq. (1) still has no validity at long evolution times and no physical justification at any time. Finally, we have no justification of the linear function $A=f(B)$ and no way of predicting its equation as a function of temperature. In the next section, we therefore try to improve our ability to predict the rate of SSA decrease by using theories of grain coarsening.

IV. THEORETICAL APPROACH

Interfacial surfaces are common in snow, either between air and ice or between two ice crystals. Seasonal snowpacks are indeed divided media composed of entangled snow grains. Their densities range from 0.01 for freshly deposited dendritic snow to 0.5 for hard windpacked snow.[7] Their SSA ranges from 1580 $\mathrm{cm^2\,g^{-1}}$ for fresh snow down to less than 100 $\mathrm{cm^2\,g^{-1}}$ for very aged snow.[22] Falling snow crystals are often single crystals or clusters of a small number of single crystals. Sintering occurs in snow together with grain coarsening and the resulting snow grains are usually polycrystals.[11,29] As a consequence, some grain boundaries exist between neighboring single crystals of different orientations.

The interfacial energy associated with the interface between two distinct media increases the free energy of the system, F. Morphological transformations spontaneously tend to minimize F. Under thermal and mechanical equilibrium, in the absence of impurities and other sources of interaction, the evolution is driven by the minimization of the total interfacial energy[30] and thus of the total interfacial area. If, as a simplification, snow crystals are considered spherical, this area increases with the grain curvature. The question of predicting the evolution of the total interfacial energy becomes that of predicting the evolution of the grain curvatures and thus of the grain sizes.

Materials scientists have dedicated many efforts to decipher the problem of grains coarsening[31] since it strongly impacts the properties of ceramics and metal alloys and hence their fabrication processes. Duval[32] and Gow[33,34] successfully applied these theories to ice and deep firn of density greater than 0.5. We are not aware of any attempt to apply theories of grain coarsening to dry seasonal snow. Section IV A recalls these theories, Sec. IV B shows that Eq. (1) can be derived from these theories and Sec. IV C concludes on their predictive value in the case of snow evolving under isothermal conditions.

A. Snow coarsening theories

The first grain coarsening theories addressed the case of dense materials, because only one phase has to be considered. The driving force is then the minimization of the energies of grain boundaries. Grains grow by grain boundary motion to minimize their overall curvature. Burke and Turnbull[35] proposed a simple model to predict the time dependence of the mean grain size in any dense material. They assumed that boundary motion is driven by curvature only. A curved interface undergoes a pressure P that depends on its radius of curvature r according to the equation of Laplace

$$P=\frac{2\gamma}{r}, \tag{2}$$

where γ is the interfacial energy. Under pressure P, grain boundaries move with a velocity v proportional to P. They claimed that $P=\mu v$, where μ is a constant multiplicative coefficient. The radius of curvature, r, of the boundary, is assumed proportional to R, the mean radius of an individual grain, so that $r=\lambda R$. The interfacial energy γ is assumed to be independent of the grain boundary. Finally, they give the growth rate of any grain proportional to the grain boundary velocity

$$\frac{dR}{dt}=\frac{2\mathrm{C}}{\mu\lambda}\frac{\gamma}{R}, \tag{3}$$

where C is a constant. Integrating Eq. (3) and identifying R with $\overline{R}$, the mean radius of the grain distribution, they obtained the following equation

$$\overline{R}^2-\overline{R}_0^2=Kt, \tag{4}$$

where $\overline{R}_0$ is the initial mean grain radius and $K=4\mathrm{C}\gamma/\mu\lambda$ is the growth rate. This model does not account for the dispersion of the grain sizes, and implicitly assumes that the mean grain radius evolves like the radius of a grain whose initial size would be $\overline{R}_0$. Equation (4) has been derived using restrictive hypotheses and many studies have attempted to make a more realistic description of a material.

Mean field models were proposed[36–38] to describe the interactions between grains of different sizes. Each grain of a distribution of grains was subjected to an environment whose properties represent the average effect of the overall distribution on that grain. The law of boundary velocity and the shape of the grain size distribution are linked. Feltham[36] used a log-normal grain size distribution and solved for the law of boundary motion. Hillert[37] suggested a curvature-driven law

Downloaded 01 Jun 2004 to 132.239.1.230. Redistribution subject to AIP license or copyright, see http://jap.aip.org/jap/copyright.jsp

of boundary velocity and solved for the corresponding grain size distribution. Louat[38] assumed that boundaries moved randomly and also solved for the grain size distribution. Their hypotheses are fairly distinct but, strikingly, they all found that the mean grain radius followed Eq. (4).

These models still did not account for topological constraints on grain growth, or for anisotropy of the interfacial energy. Therefore, Srolovitz *et al.*[39] and Anderson *et al.*[40] generated a grain network and studied its evolution using Monte Carlo simulations. They showed that the mean grain radius followed Eq. (5)

$$\overline{R}^n - \overline{R}_0^n = Kt, \tag{5}$$

where n is called the growth exponent. This result is very similar to Eq. (4), but they obtained values of n greater than 2.

All previous theories apply to dense, pure materials. Real materials, however, often contain impurities or porosity likely to interfere with the grain coarsening process.[41] The case of porous materials has been considered by Greskovitch and Lay[42] and Lange and Kellett,[43] who proposed a two-step mechanism. The porosity is the ratio of the gas phase volume to the volume of the overall material. Grain boundaries in very porous materials of porosity higher than 0.4 are usually located at the necks between grains. Boundary motion implies an increase in its surface area and is energetically unfavorable. The first step thus consists in the filling of the neck by vapor, surface, grain boundary, or lattice diffusion. The grain boundary can then move across the smaller grain and reduce its surface area at the same time. This second step is the usual mechanism of grain boundary migration encountered in dense materials. If the first step is quick, the second step is rate limiting and all happens as if the material was dense. Otherwise, the coarsening rate depends on the first step kinetics. From qualitative considerations, the authors suggested that Eq. (5) should apply with $n=2$ or $n=3$, when the rate limiting process is lattice or surface diffusion, respectively.

Readey[44] looked at the problem of grain coarsening from a different angle, excluding any mechanism of grain boundary migration. He proposed to interpret the grains growth rates observed in porous TiO_2 ceramics within the theoretical framework developed for Ostwald ripening studies. Ostwald[45] observed that solid particles dispersed in their melt underwent global coarsening, the largest ones consuming the smallest ones. Readey[44] showed that the case of solid particles dispersed in a gas phase was analogous, replacing the solute concentrations with the gas partial pressure. We therefore describe the theories of Ostwald ripening as they were given for liquid–solid systems.

Lifshitz and Slyozov[46] and Wagner[47] independently gave the first theoretical description of Ostwald ripening, hereafter called the LSW theory. The LSW theory likens the particles to spheres and is concerned with solid–liquid exchanges. The solute concentration far away from the particles is assumed to be constant. Since the equilibrium concentration is related to curvature by Kelvin's Law, small particles melt and large particles grow. Surface is assumed to be rough, so that all molecules that impinge on the surface become incorporated. In that case, the growth rate is linearly related to the surface supersaturation. Finally, the theory assumes that the solid volume fraction tends to zero, so that the liquid phase diffusion field around a given particle is not perturbed by the presence of the others. Under these conditions, they demonstrated that after a transient stage, the system reaches a steady-state regime. When this steady state is controlled by liquid phase diffusion, it is characterized by (i) a time-invariant particle size distribution (PSD) when normalized to the mean grain size, (ii) no particle greater than twice the average grain size and (iii) Eq. (5) with $n=3$ for the mean grain size evolution. When the surface kinetics control the rate of coarsening according to a rough interface model, the conclusions are similar but $n=2$ and the maximum grain size is 1.5 times the average grain size.

Many attempts were dedicated to extend the LSW theory to finite solid volume fractions.[48–52] They again confirmed the validity of Eq. (5), even at solid volume fractions as high as 0.3, the growth rate K being a function of the solid volume fraction ϕ. Finally, De Hoff[53,54] showed that Eq. (5) still holds for nonspherical particles and that n is not affected by the particles shape.

It is remarkable that these theories all yield Eq. (5) to describe the evolution of the mean grain radius, the only difference between them being the predicted value of n. It probably arises from the fact that they also have in common Kelvin's Law as the driving force of the coarsening process. If any of these theories does apply to snow, our experimental Eq. (1) should be consistent with the general theoretical Eq. (5). We should then be able to determine the value of n in the case of the coarsening of snow grains and possibly use it to identify which theoretical formalism is most suitable.

B. Snow metamorphism and the equations of grain growth theories

Our objective is to test whether we can reproduce our experimental observations with the theoretical Eq. (5), that gives the rate of evolution of the mean grain radius. The difficulty is to convert it into a convenient form to describe the SSA evolution instead of the mean grain radius evolution. This is all the more delicate that the definition of the grain radius of nonspherical grains is somehow arbitrary.[33,55] For spherical ice particles of radius R_c and density ρ_{ice}, the specific surface area is

$$\text{SSA} = \frac{3}{\rho_{\text{ice}} R_c}. \tag{6}$$

For nonspherical particles, Eq. (6) should qualitatively hold if multiplied by a form factor f to account for nonsphericity. Assuming that the form factor is time independent, Eq. (5) can be transformed into

$$\text{SSA}^n = \frac{\text{SSA}_0^n}{1 + K\text{SSA}_0^n \left(\frac{\rho_{\text{ice}}}{3f}\right)^n t} \tag{7}$$

with SSA_0 the initial specific surface area. Setting

Downloaded 01 Jun 2004 to 132.239.1.230. Redistribution subject to AIP license or copyright, see http://jap.aip.org/jap/copyright.jsp

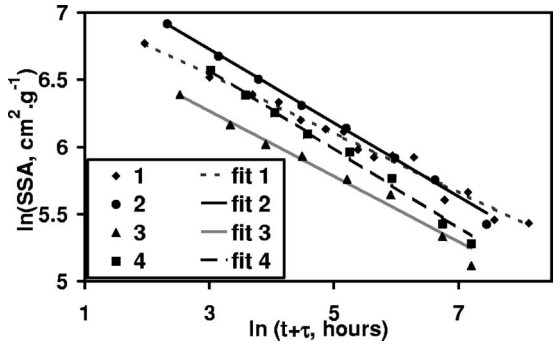

FIG. 3. Log–Log plot of the experimental results fitted by Eq. (9). All evolutions show essentially similar slopes.

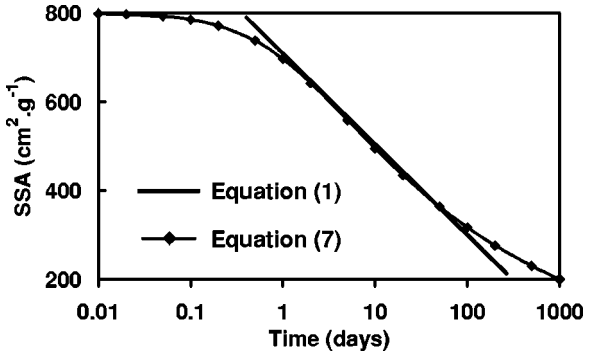

FIG. 4. Comparison of Eqs. (1) and (9). Here, Eq. (1) approximates Eq. (9) well for evolution times between 1 and 70 days.

$$\tau = \frac{1}{K}\left(\frac{3f}{\rho_{\text{ice}}\text{SSA}_0}\right)^n \tag{8}$$

yields

$$\text{SSA} = \text{SSA}_0\left(\frac{\tau}{t+\tau}\right)^{1/n}, \tag{9}$$

where τ and n are constants.

In spite of the apparent lack of similarity between this equation and the experimental logarithmic relationship (1), we fitted it to our data. Figure 3 shows the experimental curves of SSA decrease in logarithmic coordinates and Table III lists the fitting parameters SSA_0, n and τ. The agreement is excellent for all series. In addition, Eq. (9) also has the advantage that a physical meaning can be ascribed to the parameters SSA_0, τ and n. SSA_0 is unambiguously defined as the initial specific surface area when $t=0$, which makes the fit more constrained. The remaining adjustable parameters n and τ should be linked to physical variables by the grain coarsening theories. Before investigating this important question, we will clarify why Eqs. (1) and (9) both describe the experimental data very well.

At the time scale available to our coarsening experiments, Eqs. (1) and (9) both appear to give suitable fits, but Eq. (9) tends to zero for long coarsening times whereas Eq. (1) becomes negative, which is unrealistic. We demonstrate below that Eq. (1) is an approximation of Eq. (9) under certain conditions. Equation (9) can be rewritten as follows:

TABLE III. Coefficients SSA_0, τ and n for the best fits obtained with Eq. (7).

Expt. No.	Temperature °C	SSA_0 $\text{cm}^2\,\text{g}^{-1}$	τ Hours	n
1	−15	870	7.1	4.6
2	−15	1007	10.2	3.6
3	−15	592	12.5	4.1
4	−15	738	18.0	3.4
5	−15	515	39.7	5.0
6	−15	557	68.9	3.7
7	−4	488	37.9	4.3
8	−15	694	57.4	3.4
9	−10	386	217.5	2.8

$$\text{SSA} = \text{SSA}_0\lambda^{-1/n}\left(\frac{\lambda\tau}{t+\tau}\right)^{1/n}, \tag{10}$$

where λ is a real number. Equivalently

$$\text{SSA} = \text{SSA}_0\lambda^{-1/n}\exp\left[-\frac{1}{n}\ln\left(\frac{t+\tau}{\lambda\tau}\right)\right]. \tag{11}$$

This exponential can be expanded for $t+\tau \approx \lambda\cdot\tau$, yielding

$$\text{SSA} = \left[\text{SSA}_0\lambda^{-1/n}\left(1+\frac{1}{n}\ln(\lambda\tau)\right)\right] - \left[\text{SSA}_0\lambda^{-1/n}\frac{1}{n}\right]\ln(t+\tau). \tag{12}$$

This expression is formally identical to Eq. (1) with B and A corresponding to the brackets, but it only holds in the vicinity of $t=(\lambda-1)\tau$. Since no restriction was placed on λ, Eq. (9) can be approximated at any time $(\lambda-1)\tau$ by Eq. (1) if suitable parameters $A(\lambda)$, $B(\lambda)$ and $\Delta t(\lambda)$ are chosen. Figure 4 illustrates the correspondence between Eqs. (1) and (9): Eq. (1) is a good approximation of Eq. (9) over the time range of our experiments.

The reason why A and B are linearly related is, however, not totally clear. We propose the following qualitative arguments. Comparing the brackets that define A and B in Eq. (12) yields Eq. (13)

$$A = \frac{1}{n+\ln(\lambda\tau)}B. \tag{13}$$

Since, according to grain coarsening theories, n characterizes the physical processes that rule snow metamorphism, it is expected to be independent on the experimental conditions. Moreover, Eq. (1) is derived from Eq. (9) for $t \approx (\lambda-1)\tau$. Since all our experiments last almost 2 or 3 months, the approximation always holds in the same time interval. The value of $\ln(\lambda\tau)$ should thus vary little from one experiment to another. As a consequence, A and B should be simply related by a multiplicative coefficient. The fact that Fig. 2 shows a linear, rather than a proportionality, relationship can probably be ascribed to experimental uncertainty. Forcing the fit through the origin still yields a correlation coefficient of 0.904. These arguments are not limited to a given temperature and A and B should be related by the very same linear relationship for all temperatures. This is consistent with the

Downloaded 01 Jun 2004 to 132.239.1.230. Redistribution subject to AIP license or copyright, see http://jap.aip.org/jap/copyright.jsp

alignment of all points independently from their temperature in Fig. 2, but again these considerations are purely qualitative and should be taken with care.

Equation (1) has been shown to ensue from Eq. (5) which has been found to have a sound theoretical basis in many previous studies. This legitimates its use as a fitting equation and suggests that one of the grain coarsening theories mentioned above may help predict the rate of SSA decrease. We also stress that Eq. (9) is more adequate than Eq. (1) since it has a more general validity. One of its three parameters is identified as the initial SSA and the physical significance of the other two can possibly be determined from theory. For that purpose, we need to know whether one of the aforementioned theories is consistent with the physical mechanisms that rule snow metamorphism.

C. Theoretical prediction of the rate of SSA decrease

Predicting the rate of SSA decrease requires the knowledge of n and τ. Each grain coarsening theory shows that the average grain radius follows Eq. (5) with a specific value of n that characterizes the physical processes involved in that theory. Each theory also gives its analytical expression of the growth rate K that allows the prediction of τ from Eq. (8). The parameter τ can be determined from a given theory only if n coincides with the value predicted by this theory. This condition is necessary but not sufficient, because many theories yield the same value for n. Since Eq. (5) has been shown to fit our experimental curves of SSA decrease, n can be determined for isothermal snow metamorphism from our data. We then use it to discuss the applicability of each theoretical framework to the determination of τ in snow.

It is remarkable in Fig. 3 that all curves have essentially similar slopes. This in fact corresponds to identical n values and Table III tells us that n is about 4. Unfortunately, none of the aforementioned theories yields $n=4$. We notice that $n \approx 3$ in series 7, but this result should be considered carefully since Legagneux *et al.*[26] reported snow heterogeneity problems within this series. It seems therefore unlikely that one of these theories could be used without adjustments to express τ and predict the rate of SSA decrease.

Some grain coarsening theories have also been applied successfully to ice. Duval and Lorius[56] and Duval[32] have shown from experimental observations that grain coarsening occurs in dense ice and that the average grain radius follows Eq. (5) with $n=2$. They interpreted this in accordance with the mean field theory developed by Hillert[37] for dense materials where coarsening minimizes curvature by grain boundary migration. Gow[33,34] and Alley, Bolzan, and Whillans[57] reported the very same coarsening law in firn, i.e., multiannual snow, of density as low as 0.4. This was explained by Alley, Perepezko, and Bentley,[58] with the model of Greskovich and Lay.[42] Arguing that the saturating vapor pressure of ice is very high, they concluded that intense sublimation-condensation cycles filled the necks rapidly so that grain boundary migration was still the rate-limiting step and controlled the long term evolution.

It is legitimate to wonder why seasonal snow should evolve differently from multi-annual snow and yield $n=4$ instead of $n=2$. This difference may arise from a basic reason: we do observe the same material, but not the same morphological changes. The term ''grain,'' in firn studies, refers to a single crystal. In firn, as explained above, the grains grow by grain boundary migration to reduce the inter-grain interface. The surface area that shrinks is that of the ice-ice interface. We measure the specific surface area of snow. We thus follow the surface area reduction of the ice-air interface. Even if both evolutions are curvature driven, the interfaces of interest are not the same. Hence, they cannot be described by the very same theory because the mechanisms that reduce the curvature are different. We conclude that grain coarsening theories developed for dense or porous materials and that deal with ice-ice boundaries cannot help very much to model the evolution of the ice-air interface in isothermal snow.

On the contrary, our problem seems fairly close to the general LSW formalism. Metamorphism in dry isothermal snow is driven by variations in curvature according to Kelvin's law.[30] The solid volume fraction remains fairly low since fresh snow densities can be as low as 0.01 and almost always lower than 0.2. The densities of aged seasonal snow rarely exceed 0.45. Surface kinetics are involved through sublimation condensation of water vapor at the sources and sinks, respectively. Finally, it is widely assumed that water vapor diffusion dominates matter fluxes in snow[11,23,59] as is the case during Ostwald ripening. Yet we neither find $n=2$ nor $n=3$, which corresponds to the prediction of the steady-state theories of Ostwald ripening, for growth limited, respectively, by surface kinetics on a rough interface or diffusion in the vapor phase.

Many reasons can be invoked to explain why these steady-state theories of Ostwald ripening fail to reproduce the behavior of snow. (i) The geometrical assumption of disconnected spheres may be inapplicable. (ii) Surface processes are rate limiting but differ from the rough interface model. (iii) The steady-state regime has not been reached and the conclusions of the steady-state theories of Ostwald ripening do not apply. We address these hypotheses successively.

(i) Snow crystals are not spherical, especially in fresh snow. Moreover, snow crystals are not isolated but belong to a continuous network. This modifies the diffusion field around the grains and possibly the kinetics of coarsening. Accounting precisely for geometrical effects necessitates complex 3D modeling, which is far beyond the scope of this article. However, it has been shown that nonsphericity or a volume fraction of solid different from zero modify the growth rate but do not affect the growth exponent.[48,49,53,54] We thus do not think that (i) alone explains our high n values.

(ii) At high temperatures, disorder appears on the ice surface, forming what is called the quasiliquid layer.[60,61] This has at least two effects. First, the water molecules are less bonded in the quasiliquid layer, their mobility increases and the possibility of significant surface diffusion cannot be completely ruled out. Second, it lowers the free energy of formation of a stable nucleus of a new growth layer on the ice surface and allows the crystal to grow by layer nucleation.[62,63] Growth limited by surface processes other

Downloaded 01 Jun 2004 to 132.239.1.230. Redistribution subject to AIP license or copyright, see http://jap.aip.org/jap/copyright.jsp

than those described by a rough interface model could yield $n \neq 2$. For example, Cabane, Laporte, and Provost[64] investigated the kinetics of Ostwald ripening of quartz in silicic melts and reported growth exponents between 5 and 7. Among other explanations, they suggested that this could be due to interface-controlled Ostwald ripening with a surface nucleation mechanism.

We attempt to discard hypothesis (ii) by demonstrating that in snow, gas phase diffusion is more efficient than surface diffusion and that surface kinetics thus do not limit the growth rate. To prove this, we conducted another isothermal evolution with snow similar to that used in experiment 4. The only difference was that we evacuated the container so that all the evolution took place in pure water vapor, at the saturating vapor pressure of water at $-15\,^{\circ}\mathrm{C}$. These conditions, presumably, do not influence much the rate of sublimation-condensation or the rate of surface diffusion, but they increase the diffusion coefficient of water in the gas phase by more than two orders of magnitude. If diffusion is actually rate limiting, the rate of SSA decrease should be much higher under vacuum. SSA decreased in 200 h by a factor of 2 under 1 atm of air and by a factor of 10 in the absence of air. We can then consider that diffusion is rate limiting under isothermal conditions at $-15\,^{\circ}\mathrm{C}$. This is consistent with Ostwald ripening limited by diffusion. Hypothesis (ii) therefore does not explain why we find $n \approx 4$. However, we recognize that this conclusion relies on the initial assumption that the absence of air does not affect the surface processes, which still needs more support.

(iii) We now have to evaluate whether the steady-state regime is established or not, i.e., whether the scaled PSD reaches a time-stable shape. This is all the more important that analytical expressions of τ are available only under steady-state conditions. In recent experiments, Alkemper *et al.*[65] and Snyder, Alkemper, and Voorhees[50,51] observed Ostwald ripening of solid-Sn particles in a Pb–Sn liquid mixture. They conducted these experiments in conditions that carefully respected the LSW hypothesis and with various volume fractions of solid. A major issue of their work was that their experiments never reached steady state. Although they did obtain Eq. (5) with $n=3$, they cannot apply steady-state theories to derive conclusions from this value and, in particular, it cannot be concluded that gas phase diffusion was rate limiting. They demonstrated that the transient model of Akaiwa and Voorhees[49] reproduced the observed particle size distributions and growth rates remarkably well and, in any case, much better than the steady-state models. Cabane, Laporte, and Provost[64] also proposed that growth in the transient regime could explain their high growth exponents for Ostwald ripening of quartz in silicic melts. Figure 5 shows why a transient regime can be described by Eq. (5) and $n > 3$. Within the time space of a few months accessible to experiment, the fictitious experimental curve of SSA decrease does not reach the asymptotic curve of slope 1/3 but seems to reach an asymptotic curve of slope $1/n$ with $n>3$.

We thus conclude that the most likely explanation for our high values of n appears to be that steady state has not been reached. However, a better understanding of aspects such as surface processes during snow metamorphism under atmospheric conditions would help to strengthen our conclusion.

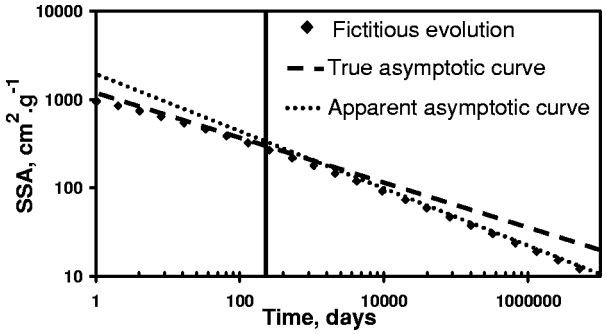

FIG. 5. Diamonds: fictitious curve of SSA decrease in log–log coordinates. Dotted line: true asymptote of slope 1/3. It is not reached within the time accessible to experiments, indicated by the solid vertical line (a few hundred days). Dashed line: apparent asymptote of slope $1/n_{\mathrm{apparent}} < 1/3$ reached after a few hundred days.

The coarsening processes are slow in isothermal snow and probably need time to reach steady state. To test the possibility that grain coarsening in our experiments did occur in the transient regime, we need to compare the PSDs at different steps of the evolution. Unfortunately, it is difficult to define a PSD in fresh snow because grains have tortuous shapes. On the other hand, curvature maps can be obtained by x-ray tomography.[66] We thus propose to use the curvature distribution rather than the PSDs. For spheres, the PSD's invariance implies the invariance of the surface curvature distribution as follows. With R_{av} the average grain radius, R_x the radius of a given grain, and x the dimensionless radius defined by $R_x = x \cdot R_{\mathrm{av}}$, the number N of grains in each size class must be related by a constant function of x to verify the time invariance of the PSD

$$\frac{N(R_x)}{N(R_{\mathrm{av}})} = f(x). \tag{14}$$

Consequently, the ratio between the surfaces S of radius of curvature R_{av} and R_x is also a function of x alone

$$\frac{S(R_x)}{S(R_{\mathrm{av}})} = \frac{N(R_x) 4\pi R_x^2}{N(R_{\mathrm{av}}) 4\pi R_{\mathrm{av}}^2} = f(x)\left(\frac{1}{x}\right)^2. \tag{15}$$

Flin *et al.*[27] used tomographic data to derive the curvature distribution at different steps of evolution of fresh snow in isothermal conditions at $-2\,^{\circ}\mathrm{C}$. We plotted their surface curvature distribution scaled by the mean grain size at various steps of evolution (Fig. 6). The trend is clear and shows that the distribution becomes more symmetric and that the maximum translates toward high radii. The curvature distribution is not constant, which we interpret as a proof that the steady-state regime has not been reached. Since metamorphism is faster at higher temperature, the PSD should reach its steady shape even more slowly at lower temperatures such as encountered in our experiments.

From this discussion, we conclude that the value $n=4$ in Eq. (5), found for the rate of decrease of snow SSA under isothermal conditions, is mainly due to the fact that steady state has not been reached. A contribution of items (i)–(iii) to

Downloaded 01 Jun 2004 to 132.239.1.230. Redistribution subject to AIP license or copyright, see http://jap.aip.org/jap/copyright.jsp

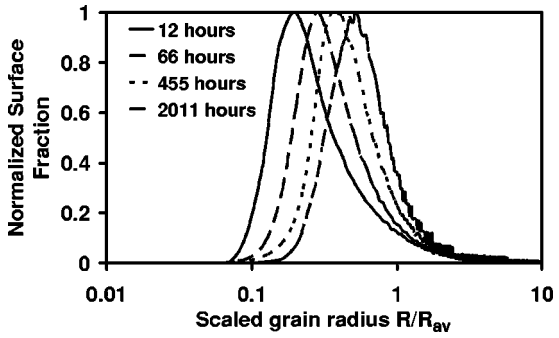

FIG. 6. Normalized surface fraction vs scaled grain radius at given times during the isothermal evolution of snow at -2 °C. All data from this figure are from Flin *et al.* (see Ref. 27). The evolution suggests that the steady-state regime for Ostwald ripening has not been reached.

explain this observation cannot be definitely ruled out, until the kinetic processes that occur on the surface of ice are better understood. Anyway, a direct prediction of the rate of SSA decrease in isothermal snow from the theories of Ostwald ripening in steady state is not possible. On the other hand, the description of the physics of snow metamorphism with the framework of Ostwald ripening in transient regime seems adequate, and this warrants further developments.

V. SUMMARY AND CONCLUSION

Experimental results on the isothermal evolution of the specific surface area of snow are presented and complement previous data by Legagneux *et al.*[26] They are well fitted by a logarithmic equation $\mathrm{SSA}=B-A\ln(t+\Delta t)$ and the linear relationship between parameters A and B, suggested by Legagneux *et al.*[26] is confirmed.

We investigated the possibility of using grain coarsening theories to shed some light on these results and to predict the rate of SSA decrease. The general properties of those theories allowed us to propose a better equation to fit the data (9). This equation holds even at long times of evolution, is locally approximated by the logarithmic Eq. (1), and one of its three parameters is readily identified with the initial specific surface area SSA_0. However, none of the theories reviewed here applies directly to snow grain coarsening.

The main physical processes involved in the decay of snow SSA are those of Ostwald ripening. Ostwald ripening theories show the existence of a steady-state regime, characterized by a time invariant PSD when scaled to the mean grain radius. The PSD invariance implies the surface curvature distribution invariance, at least for spherical particles. If these considerations apply to snow, then the data of Flin *et al.*[27] indicate that the steady-state regime was not reached after 2011 h of isothermal evolution at -2 °C. Considering the accelerating effect of temperature on metamorphism, we suggest that isothermal snow probably does not have enough time to reach the steady-state distribution within a few months. The prediction of the rate of SSA decrease under isothermal conditions thus cannot arise from the steady-state theories but would likely ensue from simulations of the transient Ostwald ripening.

Complex 3D models of transient Ostwald ripening exist but they handle disconnected spherical particles.[49] A model with realistic 3D geometry is being developed by Flin *et al.*,[27] but as mentioned above, they do not account for the limiting effect of gas phase diffusion to determine the overall coarsening rate. In future work, we therefore plan to investigate transient Ostwald ripening with a simple mean field model. Our intention is to test the ability of such a basic model to reproduce satisfactorily the experimental curves of SSA decrease. It will help to estimate the dependency of n and τ on crucial variables such as snow temperature, density, and the initial PSD.

ACKNOWLEDGMENTS

This work was supported by CNRS through Program National de Chimie Atmosphérique (PNCA). The authors thank Jean-Bruno Brzoska, Frédéric Flin, and co-workers from CEN-Météo France for making their data available prior to publication, and for stimulating discussions.

[1] S. C. Colbeck, Rev. Geophys. **29**, 81 (1991).
[2] E. Brun, E. Martin, V. Simon, C. Gendre, and C. Coleou, J. Glaciol. **35**, 333 (1989).
[3] E. Brun, P. David, M. Sudul, and G. Brunot, J. Glaciol. **38**, 13 (1992).
[4] Y. Durand, G. Giraud, E. Brun, L. Merindol, and E. Martin, J. Glaciol. **45**, 469 (1999).
[5] H. Dang, C. Genthon, and E. Martin, Ann. Glaciol. **25**, 170 (1997).
[6] C. A. Shuman and R. B. Alley, Geophys. Res. Lett. **20**, 2643 (1993).
[7] F. Dominé and P. B. Shepson, Science **297**, 1506 (2002).
[8] G. Seligman, Snow Structure and Ski Field. An Account of Snow and Ice Forms met with in Nature and a Study on Avalanches and Snowcraft (Macmillan, London, 1936).
[9] M. R. De Quervain, Association Internationale d'hydrologie Scientifique, International Association of Scientific Hydrology. Extrait des Comptes Rendus et Rapports, Assemblee Generale de Toronto 1957, Vol. 4, pp. 225–239 (1958).
[10] S. C. Colbeck, Cold Regions Research and Engineering Laboratory Research Report **313**, 1-11 (1973).
[11] S. C. Colbeck, Rev. Geophys. Space Phys. **20**, 45 (1982).
[12] C. Raymond and K. Tusima, J. Glaciol. **22**, 83 (1979).
[13] E. Brun, Ann. Glaciol. **13**, 22 (1989).
[14] S. C. Colbeck, J. Geophys. Res. **88**, 5475 (1983).
[15] M. Sturm and C. S. Benson, J. Glaciol. **43**, 42 (1997).
[16] S. C. Colbeck, Water Resour. Res. **22**, 59S (1986).
[17] D. Marbouty, J. Glaciol. **26**, 303 (1980).
[18] H. Schwander, B. Mayer, A. Ruggaber, A. Albold, G. Seckmeyer, and P. Koepke, Appl. Opt. **38**, 3869 (1999).
[19] W. Abdalati and K. Steffen, J. Glaciol. **44**, 523 (1998).
[20] E. M. Arons and S. C. Colbeck, Rev. Geophys. **33**, 463 (1995).
[21] M. R. Albert, Ann. Glaciol. **23**, 138 (1996).
[22] L. Legagneux, A. Cabanes, and F. Domine, J. Geophys. Res. **107**, 4335 (2002).
[23] S. A. Sokratov, Cold Regions Sci. Technol. **33**, 263 (2001).
[24] A. Cabanes, L. Legagneux, and F. Domine, Atmos. Environ. **36**, 2767 (2002).
[25] A. Cabanes, L. Legagneux, and F. Domine, Environ. Sci. Technol. **37**, 661 (2003).
[26] L. Legagneux, T. Lauzier, F. Domine, W. Kuhs, T. Heinrichs, and K. Techmer, Can. J. Phys. **81**, 459 (2003).
[27] F. Flin, J. B. Brzoska, B. Lesaffre, C. Coléou, and R. A. Pieritz, Ann. Glaciol. **38**, (2004) (in press).
[28] F. Flin, J. B. Brzoska, B. Lesaffre, C. Coléou, and R. A. Pieritz, J. Phys. D **36**, 1 (2003).
[29] S. C. Colbeck, CRREL Rep. **97-10**, 1–17 (1997).
[30] S. C. Colbeck, J. Glaciol. **26**, 291 (1980).
[31] H. V. Atkinson, Acta Metall. **36**, 469 (1988).
[32] P. Duval, Ann. Glaciol. **6**, 79 (1985).
[33] A. J. Gow, J. Glaciol. **8**, 241 (1969).

Downloaded 01 Jun 2004 to 132.239.1.230. Redistribution subject to AIP license or copyright, see http://jap.aip.org/jap/copyright.jsp

[34] A. J. Gow, Cold Regions Research and Engineering Laboratory Research Report **300**, 1-19 (1971).
[35] J. E. Burke and D. Turnbull, Prog. Met. Phys. **3**, 220 (1952).
[36] P. Feltham, Acta Metall. **5**, 97 (1957).
[37] M. Hillert, Acta Metall. **13**, 227 (1965).
[38] N. P. Louat, Acta Metall. **22**, 721 (1974).
[39] D. J. Srolovitz, M. P. Anderson, P. S. Sahni, and G. S. Grest, Acta Metall. **32**, 793 (1984).
[40] M. P. Anderson, D. J. Srolovitz, G. S. Grest, and P. S. Sahni, Acta Metall. **32**, 783 (1984).
[41] R. J. Brook, *Treatise on Materials Science and Technology*, edited by F. F. Y. Wang (Academic, New York, 1976), Vol. 9, p. 331.
[42] C. Greskovitch and K. W. Lay, J. Am. Ceram. Soc. **55**, 142 (1971).
[43] F. F. Lange and B. J. Kellett, J. Am. Ceram. Soc. **72**, 735 (1989).
[44] M. J. Readey and D. W. Readey, J. Am. Ceram. Soc. **70** (1987).
[45] W. Ostwald, *Analytische Chemie*, 3rd ed. (Engelmann, Leipzig, 1901).
[46] I. M. Lifshitz and V. V. Slyozov, J. Phys. Chem. Solids **19**, 35 (1961).
[47] C. Wagner, Z. Elektrochem. **65**, 581 (1961).
[48] A. D. Brailsford and P. Wynblatt, Acta Metall. **27**, 489 (1979).
[49] N. Akaiwa and P. W. Voorhees, Phys. Rev. E **49**, 3860 (1994).
[50] V. A. Snyder, J. Alkemper, and P. W. Voorhees, Acta Mater. **48**, 2689 (2000).
[51] V. A. Snyder, J. Alkemper, and P. W. Voorhees, Acta Mater. **49**, 699 (2001).
[52] R. N. Stevens and C. K. L. Davies, J. Mater. Sci. **37**, 765 (2002).
[53] R. T. De Hoff, Acta Metall. **32**, 43 (1984).
[54] R. T. De Hoff, Acta Metall. Mater. **39**, 2349 (1991).
[55] E. E. Underwood, Quantitative Stereology (Addison–Wesley, Reading, MA, 1970).
[56] P. Duval and C. Lorius, Earth Planet. Sci. Lett. **48**, 59 (1980).
[57] R. B. Alley, J. F. Bolzan, and I. M. Whillans, Ann. Glaciol. **3**, 7 (1982).
[58] R. B. Alley, J. H. Perepezko, and C. R. Bentley, J. Glaciol. **32**, 415 (1986).
[59] Z. Yosida, Low Temp. Sci. A **7**, 19 (1955).
[60] M. Faraday, Philos. Mag. **17**, 162 (1859).
[61] A. Döppenschmidt and H. J. Butt, Langmuir **16**, 6709 (2000).
[62] T. Kuroda and R. Lacmann, J. Cryst. Growth **56**, 189 (1982).
[63] J. Nelson and C. Knight, J. Atmos. Sci. **55**, 1452 (1998).
[64] H. Cabane, D. Laporte, and A. Provost, Contrib. Mineral. Petrol. **142**, 361 (2001).
[65] J. Alkemper, V. A. Snyder, N. Akaiwa, and P. W. Voorhees, Phys. Rev. Lett. **82**, 2725 (1999).
[66] J. B. Brzoska, B. Lesaffre, C. Coléou, K. Xu, and R. A. Pieritz, Eur. Phys. J. A **7**, 45 (1999).

Downloaded 01 Jun 2004 to 132.239.1.230. Redistribution subject to AIP license or copyright, see http://jap.aip.org/jap/copyright.jsp